International Journal of Nanomedicine

Dovepress
open access to scientific and medical research

Open Access Full Text Article

ORIGINAL RESEARCH

An AFM-Based Nanomechanical Study of Ovarian Tissues with Pathological Conditions

This article was published in the following Dove Press journal:
International Journal of Nanomedicine

Arian Ansardamavandi[1]
Mohammad Tafazzoli-Shadpour[1]
Ramin Omidvar[2]
Fatemeh Nili[3]

[1]Department of Biomedical Engineering, Amirkabir University of Technology, Tehran, Iran; [2]Faculty of Biology, Centre for Biological Signalling Studies (BIOSS), Albert Ludwigs University Freiburg, Freiburg, Germany; [3]Department of Pathology, Tehran University of Medical Sciences, Tehran, Iran

Background: Different diseases affect both mechanical and chemical features of the involved tissue, enhancing the symptoms.

Methods: In this study, using atomic force microscopy, we mechanically characterized human ovarian tissues with four distinct pathological conditions: mucinous, serous, and mature teratoma tumors, and non-tumorous endometriosis. Mechanical elasticity profiles were quantified and the resultant data were categorized using K-means clustering method, as well as fuzzy C-means, to evaluate elastic moduli of cellular and non-cellular parts of diseased tissues and compare them among four disease conditions. Samples were stained by hematoxylin–eosin staining to further study the content of different locations of tissues.

Results: Pathological state vastly influenced the mechanical properties of the ovarian tissues. Significant alterations among elastic moduli of both cellular and non-cellular parts were observed. Mature teratoma tumors commonly composed of multiple cell types and heterogeneous ECM structure showed the widest range of elasticity profile and the stiffest average elastic modulus of 14 kPa. Samples of serous tumors were the softest tissues with elastic modulus of only 400 Pa for the cellular part and 5 kPa for the ECM. Tissues of other two diseases were closer in mechanical properties as mucinous tumors were insignificantly stiffer than endometriosis in cellular part, 1300 Pa compared to 1000 Pa, with the ECM average elastic modulus of 8 kPa for both.

Conclusion: The higher incidence of carcinoma out of teratoma and serous tumors may be related to the intense alteration of mechanical features of the cellular and the ECM, serving as a potential risk factor which necessitates further investigation.

Keywords: ovarian tumors, tissue elasticity, atomic force microscopy, cellular and extra cellular matrix components

Introduction

The state of health and disease among organs and tissues is defined in the cellular level. The initiation and progression of the pathological conditions are characterized by alterations in the function of biological cells, most notably due to environmental incentives. Cancer is an example that alterations in the function of cells due to mutations in cell proteins and transitions such as epithelial–mesenchymal transition cause tumor initiation, and in later stages invasion to healthy tissues through intravasation and extravasation. The function and behaviors of cancerous cells continuously change to form a new stage of cancer. Such adaptation includes physical aspects of the cell body such as mechanical properties. To invade, cancer cells need to pass through the extracellular matrix (ECM) and endothelial junctions, enter blood vessels and travel to other tissues. This requires highly deformable cells

Correspondence: Mohammad Tafazzoli-Shadpour
Amirkabir University of Technology, No. 350, Hafez Ave, Valiasr Square, Tehran, Iran
Tel +98 02164542385
Email Tafazoli@aut.ac.ir

submit your manuscript | www.dovepress.com
DovePress
http://doi.org/10.2147/IJN.S254342

with enhanced motility. Cancer cells are known to be softer and more deformable than normal cells, and they generate higher traction forces and stronger stress fibers that enhance motility.[1–3] Hence, alterations in mechanical properties of cancer cells are correlated with the biological and biochemical events in the cascade of cancer and can be used as biomarkers to distinguish cancer progress.[4–6]

Young's modulus of elasticity quantifies cell elasticity through the correlation between the applied force and deformation and its alterations can be used to describe the state of cell malignancy among cancer cells.[6] This parameter can be estimated by nanoindentation techniques such as atomic force microscopy (AFM) through the relationship between indentation force and the intended distance,[7] application of aspiration pressure on the suspended cell body and evaluation of cell deformation in micropipette aspiration technique,[8] or other techniques.

AFM technique has been widely used for quantifying topography of the surface and mechanical properties of materials, as well as biological samples.[9–11] A growing body of in vitro studies has mechanically characterized different cancer cell lines or cells extracted from cancerous tissues of different stages of several types of cancer.[12] More recently, due to the advantage of AFM to probe very locally, mechanical characterization has been performed on sections of cancerous tissues obtained from patients to study cellular and non-cellular parts of cancerous tissue,[13] indicating noticeable softening of cellular portions compared to normal tissues.[14,15]

Using AFM, we previously characterized layered sections of breast cancer tissues and compared them to those of normal breast tissues and distinguished differences among elastic moduli between cellular and fibrous parts of diseased and normal tissues.[4] Despite a range of studies on this issue, there is still a lack of investigation on comparison of mechanical properties of cellular and fibrous parts of tumorous tissues for different types of cancer and diseases. This is especially interesting when specific tissues with different known types of tumor generation are studied such as ovarian tissue. Ovarian cancer which initiates in the ovaries, fallopian tubes, and peritoneum causes higher mortality than any other cancer of the female reproductive system mainly due to the lack of effective early screening and diagnosis.[16]

Alterations in mechanical properties of tissues during disease initiation and progression are mostly due to abnormal adjustments in ECM synthesis and structure,[17,18] through irregular sedimentation of ECM, matrix crosslinking, or matrix degradation. Since ECM is synthesized and organized by cells, any pathological condition that affects cell behavior might influence ECM contents and structures.[12,19,20] As an example, it has been shown that the ovarian tissue of patients with diseases such as polycystic ovary syndrome has higher shear modulus than healthy tissue measured by magnetic resonance elastography.[21] While ECM fibers are synthesized by cells, cell behavior is mutually affected by the microenvironment due to external stimuli transferring physical signals to the cell body. In cancer progress, it has been shown that the adhesiveness of ovarian carcinoma cells directly depends on ECM components.[22] In vitro studies have shown the influence of physical and structural properties of substrates on the behavior of seeded cells, as cells show better proliferation and differentiation behaviors by adapting physical properties of the substrate similar to those of ECM of the original tissue.[23–25] Hence, the cell–ECM interaction and dependency necessitate study of both cell and non-cellular parts of tissues in health and disease.

In addition to cancer, it has been reported that other diseases cause changes in physical properties of cells like asthma.[26] Lung parenchymal diseases lead to chemically and physically different tissues with changes in matrix stiffness leading to the altered mechanical forces on cells, which in turn may cause cellular remodeling.[27] While malignant lesions of some organs such as thyroid, breast, prostate, and bladder have a stiffer microenvironment, tissues of ovarian and kidney malignant lesions tend to be softer;[28,29] however, all cancerous cells are reported to be softer compared to the normal ones.[30,31] Benign tumors are reported to have an average stiffness between malignant and healthy lesions.[32]

Ovarian tissue is a proper candidate for the study of changes in tissue and cell elasticity values related to the disease development since there are diverse types of ovarian tumors with possibly different mechanical properties depending on the disease character and progress. Hence, in this study, we examined the extent of changes on mechanical properties of cellular and non-cellular parts of diseased ovarian tissues with different types of tumors and cysts.

Depending on the cell type of origin, ovarian cystic neoplasms are grouped as epithelial tumors (mucinous and serous), germ cell tumors (mature teratoma and immature teratoma), sex cord-stromal tumors with lowest incidence, and other tumors.[33] Among benign ovarian neoplasms, serous and mucinous cystadenomas and mature cystic teratoma are the most common.[34,35]

Ovarian mucinous and serous cystadenoma are benign tumors with different gene expressions in adhesion molecules, matrix metalloproteinases, and tumor suppressor gene (p53).[36,37] With progress along different pathways, serous cystadenoma is thought to arise from a cortical inclusion cyst, but ovarian mucinous tumors, which are bigger, arise from the surface epithelium of the ovary.[38,39] Teratoma is referred to germ cell tumors that are composed of several different types of tissue derived from two or three embryonic layers and comprises approximately 20% of all ovarian neoplasms. The majority of these tumors are mature cystic teratomas or dermoid cysts composed of mature elements.[40,41] Endometriosis is a common gynecologic disease, in which endometrial tissue composed of endometrial stroma or endometrial-type glandular epithelium is found outside the uterus. Based on clinical findings, uterosacral ligament and ovaries are the most frequent sites of this condition.

Numerous studies have focused on the identification of ovarian tumors and their diagnostic markers;[42,43] however, mechanical properties of cellular and fibrous parts of ovarian cancerous tissues have not been considered as a possible assistive biomarker to distinguish between different types of tumors or between primary ovarian carcinoma and metastatic one. Disorders or variations in the microenvironment due to disease pathogenesis and progression can affect the content and organization of cell cytoskeleton and molecular organization, resulting in altered mechanical properties.[18,44,45] Hence, nano-scale evaluation of mechanical characteristics of cellular and fibrous parts of cancerous tissues can indicate the biological state of the disease both in terms of cancer type and stage of progress.

In this study, the elastic modulus of various ovarian diseased tissues including three non-malignant tumors having different origins (mucinous cystadenoma, serous cystadenoma, and mature teratoma) and one non-tumorous (endometriosis) was evaluated using AFM. The mechanical characterization was carried out by evaluating Young's modulus of elasticity of both cellular and non-cellular parts of tissues to describe the extent of change in mechanical properties on tissues caused by the state of disease. Using K-means and fuzzy C-means algorithm, the data were categorized to "naturally" distinguish between cellular and fibrous parts of tissues, as previously we applied on the breast tissue.[4] A deterministic approach to label data into cellular or ECM categories aside from AFM is not possible; hence, we implemented clustering algorithms to achieve unbiased categorization. Numerical calculations were compared with pathological examinations by histopathological staining method.

Materials and Methods

Examination of ovarian tissue elasticity was performed on four different ovarian-related diseases. For each disease, samples of ovarian tissues of patients in the age range of 40–50 years old were examined with informed consent with ethical approval. The left ovarian tissues of these patients were extracted by surgery due to complications and tissue samples were provided by continuous supervision of a pathologist. The elastic moduli of different locations of tissue sections were quantified by AFM. The coordinates of indented locations were recorded during experiments. By using a mathematical calculating method, elasticity histograms were obtained and data were clustered by K-means as well as Fuzzy C-means algorithms to distinguish between elastic moduli of cellular and non-cellular zones. Accordingly, the average values of elastic moduli of cellular part and ECM were calculated. Additionally, using histopathological staining on the indented tissue samples, different parts of samples were identified. Results were compared statistically to reveal the effects of tumor-related ovarian diseases on elastic moduli of different parts of ovarian tissue. Figure 1 shows the experimental approach with a schematic representation, as well as the experimental approach for the treatment of a typical sample of mature teratoma.

Tissue Preparation

Samples of ovarian tissue were obtained during surgery of female subjects with different ovarian-related diseases with written informed consent of the patient, by supervision of an expert oncologist according to the procedure regarding experiments involved human subjects, approved by Ethical Committee, Cancer Research Center, Cancer Institute, Tehran University of Medical Sciences in accordance with Declaration of Helsinki,[46] and published protocols.[47,48] The biopsy specimens were investigated by an expert pathologist and smooth uniform samples with best features and no physical damage were chosen. For AFM tests, samples with 0.3 × 1 × 1.5 cm were carefully cut and the rest of the samples were used for pathological examinations. Test samples were examined by the pathologist and were categorized as endometriosis, mucinous cystadenoma, serous cystadenoma, and mature teratoma.

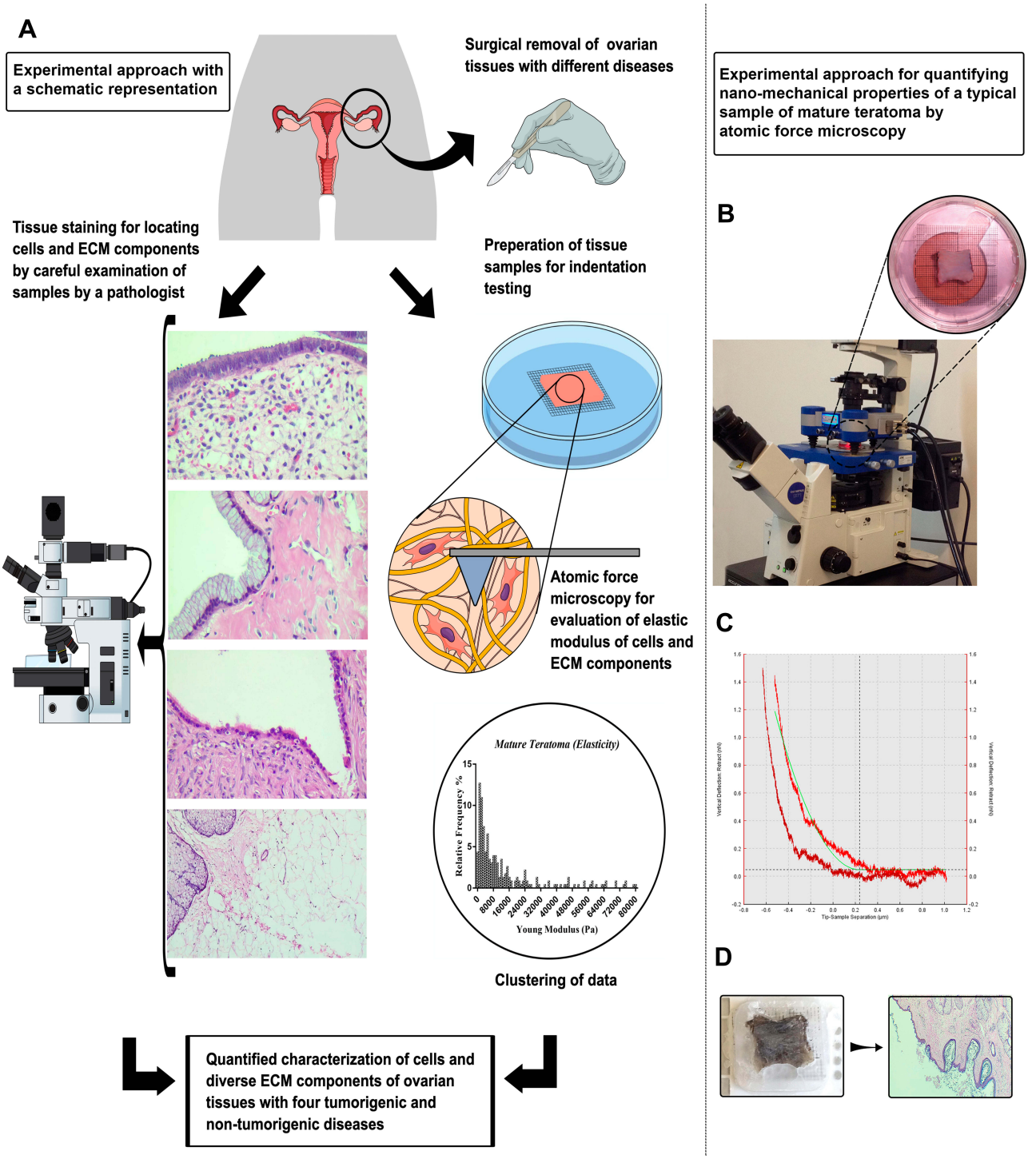

Figure 1 A representation of experimental approach. (**A**) Schematic representation of the study. (**B**) AFM measurement of the mature teratoma ovarian tissue sample, the tissue was tested while adhered to a graded plate to identify the approximate location of AFM measurement with a specific dimension of (0.3 × 1 × 1.5 cm) in DMEM solution. (**C**) The obtained data of AFM measurements. AFM tip pushes down the tissue containing cells and ECM documenting the indentation depth (μm) versus force (nN) generated by pushing down the section. This result was used for obtaining elasticity according to the fundamental equations. (**D**) The image represents the sample which was prepared for histopathological staining after AFM indentation (top), and the histopathological stained section of mature teratoma (bottom).

Samples were kept in DMEM solution at 4°C prior to the indentation tests which were being performed no longer than 6 hours after biopsy in order to prevent any tissue destruction.

AFM Experiment

To better locate the indentation sites for further analysis, in addition to AFM probe location, a graded transparent plate was placed under the petri dish containing samples that

were pasted on them by a biocompatible glue, defining the initial location and direction of continuous indentation path.[4] A Nanowizard3 atomic force microscope (JPK Instruments AG, Germany) was used in force spectroscopy mode while samples were kept in DMEM solution. Samples mounted on the stage were indented by CSC17/noAl cantilevers (MikroMasch, USA) with normal spring constant of 0.15 N/m. The cantilever spring constant was calculated with the thermal noise method.[49]

There is a wide range of AFM cantilevers for probing, including those with spherical and sharp tips. While due to the larger contact area, spherical tips provide more accurate estimate of elastic moduli, sharp tips provide higher spatial resolution. Since our aim was to discriminate the cellular and non-cellular parts of the tissue, low contact area was a key factor in order to ideally indent either cellular or non-cellular part in a force cycle. The higher spatial resolution of sharp probes provides the opportunity to cluster data more accurately. Since our primary interest was to investigate the relative effects of different diseases on mechanical properties of the tissue, and not the absolute values of elastic moduli, sharp tips were utilized in this study.

AFM can measure the elastic modulus of underlying tissue by two means of applying a preset force or deformation at a defined speed onto a surface. To achieve an optimized resolution, we used the force mode with a predefined force of 1.5nN applied by the cantilever for one second after lowering to the contact point of the samples as the reference position. The cantilever was returned to the initial position and the force-displacement data were recorded in both directions. At least 20 locations in each sample were probed, among each, 30 points were indented in an area of 30×30 µm. The spatial position of each indentation site was carefully located for histopathological analysis of that site. Since to some extent, the AFM results depend on the parameter sets and experimental conditions,[50,51] we used the same parameters and conditions for all experiments (Table 1). Setting these parameters and selecting a low speed of the probe for a better evaluation of elastic moduli,[50] a reliable comparison of elasticity values among different parts of tissue was possible.

Table 1 Representing Different AFM Features and Preset Conditions for Analyzing Elasticity of Ovarian Samples with Different Pathological Conditions

Parameters Set	Values
Applied constant force	1.5 nN
Cantilever speed	1 (µm/s)
Maximum indentation depth	2 (µm)
AFM tip contact time	1 s

Evaluation of Young's Modulus

The difference between the deflection of the cantilever's tip (d) and the position of piezoelectric crystals (Z) defines the depth of indentation (δ) as:

$$\delta = (d - d_0) - (Z - Z_0) \quad (1)$$

where d_0 and Z_0 correspondingly indicate cantilever deflection and the piezoelectric position when the tip contacts tissue surface.

Based on the spring constant of the cantilever, the tip deflection is related to the applied force. Hence, the force was applied during continuous recording of the tip deflection, and the Young's elastic modulus of the indented site of the tissue was calculated using the resultant force-displacement data and application of the Hertz model, modified by the shape of cantilever tip.[14,52]

$$F = \frac{2\tan\alpha}{\pi\left(1-\mu_{sample}^2\right)} E_{sample}\delta^2 \quad (2)$$

Parameter α represents half value of the cone angle of the tip that was 20° in this study. Parameters δ and F, respectively, show the indentation depth and the applied force, respectively. Moreover, µ indicates the Poisson ratio of the indented tissue considered to be 0.5 due to the assumption of incompressibility of soft biological tissues.[53] Substituting Equation 1 in Equation 2, a linear function is derived (Equation 3) by which the slope of the line represents the Young's modulus of indented sites.[54]

$$F^{1/2} = \left[\frac{2E_{sample}\tan\alpha}{\pi\left(1-\mu_{sample}^2\right)}\right]^{1/2}(Z-d) - \left[\frac{2E_{sample}\tan\alpha}{\pi\left(1-\mu_{sample}^2\right)}\right]^{1/2}(Z_0-d_0) \quad (3)$$

The calculated values of Young's modulus are usually represented in histogram forms when the horizontal axis shows the calculated Young's moduli and the vertical axis indicates the frequency of occurrence (or relative frequency as the normalized value to the total frequency).[55]

Clustering Algorithm

The indented parts of ovarian tissues contained cellular, fibrous, and other structural features which could not be

distinguished during nanoindentation. Hence, a wide range of values of elastic modulus was observed in the histogram. Since we hypothesized that elastic moduli of these parts were different for each specimen, we applied clustering algorithms to categorize data and naturally distinguish the number of clusters of data of elastic moduli. These clusters could be biologically meaningful such as cellular, fibrous, luminal ducts, etc. Hence, K-means clustering algorithm was used to classify experimental data into numbers of clusters to distinguish the elastic properties of different parts of tissue in such a way that there were maximum similarities between values of members of each cluster, while the differences between center of clusters were maximized.[56] In other words, the measured data were divided into clusters such that the data within each cluster were as similar as possible, while the data in different clusters were as dissimilar as possible. Using this method, we avoided to predefine categories for elastic modulus of cellular and non-cellular parts of the diseased tissues and allowed an unbiased classification and examined whether these categories were biologically meaningful.

The result of clustering varies by change in the number of clusters; hence, a main challenge of clustering algorithm is that the number of clusters is rarely known. To overcome this problem, the K-means approach can be used accompanied by available methods to estimate the number of clusters such as statistical indexes, variance-based methods, information theory, and fit methods.[57] A number of approaches utilize indexes comparing within-cluster distances with between-cluster distances to decide a criterion to select number of clusters,[58] including elbow and silhouette methods. These two well-balanced methods have proved a good performance in experiments.[59,60]

The elbow method evaluates the clustering algorithm with stepwise increase of number of clusters from 2 and calculates the average value of each cluster and the squared sum of the distances between centroid of the cluster, and within-cluster sum of squares (WCSS) according to the number of clusters. By increase of number of clusters, the WCSS value decreases markedly until reaching a plateau which defines the optimized value of number of clusters. In silhouette method, the difference between the within-cluster tightness and separation from the rest is calculated. The largest average of the difference, over different number of clusters, indicates the best number for clustering data.[57] We used both methods through MATLAB to obtain the best number of clusters, and results were considered reliable if numbers of clusters using two methods were the same.

To compare different methods of clustering, fuzzy C-means clustering tool which was performed in our previous study for clustering elastic moduli of normal and carcinoma breast tissues was also performed.[4]

Membership Grade

By determining the proper number of clusters using MATLAB Logic Toolbox, K-means clustering was used as a partitioning method. The function K-means divides data into k-limited clusters by returning the index of the cluster to which it allocates each observation. In comparison, the fuzzy C-means algorithm was also utilized to allocate data to clusters through calculation of membership grades which are numbers between [0,1]. After defining the number of clusters for samples of each ovarian disease, the cumulative center of the data in each cluster was calculated as the Young's modulus of samples assigned to that cluster.

Histopathologic Assessment

Samples were stained for pathological observation after mechanical characterization to compare the calculated elastic moduli with histological status of the indented sites. The samples underwent hematoxylin–eosin (H&E) staining according to the published protocols.[61,62] The stained samples were investigated by the pathologist and the cellular and fibrous sites were distinguished and compared to those of indented sites.

Statistical Analysis

Data were presented as mean ± standard error of the mean (SEM). At least ten samples were examined for each related ovarian tissue diseases. The number of measurements in each sample was at least 180 different points which were selected randomly. To compare elastic moduli of cellular and fibrous (ECM) locations among samples of different ovarian diseases, one-way ANOVA was performed for verification of statistical significance. Additionally, to compare samples of each disease, Bonferroni's multiple comparison test was performed. The P values for statistical significance were set to be less than 0.05.

Results

According to the histopathological staining of biopsy samples, four different ovarian tissue-related diseases were recognized and examined. After indentation tests on different locations of samples of four ovarian diseases, elasticity histograms were plotted in logarithmic scale to better compare elastic moduli of different parts of

heterogeneous tissues. Figure 2A–D shows plots of elasticity histograms of all samples of ovarian-related diseases. Results indicated marked differences among the ranges of elastic moduli described by histograms among subjects with four ovarian-related diseases. For mature teratoma, the indented sites were in the elasticity range of up to 80 kPa, at least 4-folds more than those of other groups. For samples with serous cystadenoma, Young's modulus values were less than 12 kPa, having the lowest range of elastic moduli compared to studied diseases. These results indicate that mature teratoma elasticity profile has the highest heterogeneity and the stiffest microenvironment. By the opposite trend, serous samples were the softest samples among all groups. For samples with endometriosis and mucinous cystadenoma, the ranges of obtained elastic moduli were almost similar, up to 20 kPa. However, the relative frequency of occurrence among the range of obtained elasticity was noticeably different between them. The highest frequency of elastic modulus was for 1000 Pa data for endometriosis and mucinous cystadenoma, with 30% and 20% of occurrence, respectively. Although the histogram for serous cystadenoma peaked at 500 Pa with 30% of relative frequency, the figure for mature teratoma peaked in 2000 Pa with merely 13% of occurrence, which indicates the broad and diverse elasticity profiles due to this disease (Figure 2A–D). To better compare elastic properties of ovarian tissue among four diseased conditions, the average elastic modulus of samples, regardless of indentation locations, was measured and compared among four diseased groups (Figure 2E).

Considering both cellular and non-cellular parts, results of average values of elastic moduli indicated that by far the stiffest tissue was mature teratoma, with the average of 14 kPa, and the softest ones were serous tumors with the average elastic modulus of 1.6 kPa (Figure 2E). The other values were 3.5 and 2.1 kPa for mucinous tumors and endometriosis, respectively (Figure 2E). Although the statistical results illustrate no significant difference between the average elasticity of serous, mucinous, and endometriosis tissues, exception is samples of mature teratoma with elastic moduli stiffer than that of others ($P<0.05$).

Since the elasticity histograms show variations with increased elastic modulus, the obtained data were clustered using K-means clustering algorithm. Using both elbow and silhouette methods, the optimized number of clusters was calculated and found to be three and four depending on disease conditions (Figure 3) (data not shown for silhouette method). This indicates that the obtained data does not belong to a single group, and while for the broad range of obtained elasticity in mature teratoma this number is calculated four, the stiffness variation of endometriosis, serous, mucinous should be categorized in three different regions, all indicating different parts in a tissue with a specific disease. Considering pathological examinations, we defined them as, cellular, extracellular matrix soft region (ECMs) indicating a region with a few cells with unparallel fibers of ovarian tissue, and the rigid one (ECMr) indicating fibrous part of tissue with parallel collagen fibers, consistent to previous studies.[4,13] For mature teratoma, another category was defined as the highly rigid extracellular matrix (ECMhr), indicating the highly rigid parts in the microenvironment of tissue which is not observed in other ovarian studied diseases, also proving that the microenvironment of mature teratoma tumors is by far stiffer than other quantified diseases (Figure 2E). We further analyzed data and used fuzzy C-means to categorize data based on the obtained number of clusters and similar results were obtained for all clusters of data of cellular and non-cellular parts. The difference between C-means and K-means clustered data was obtained insignificant.

According to the mathematical clustering calculation, the data which belong to the cellular parts of measured diseases were selected and plotted in a separate histogram. The elastic moduli of cells in measured tumors showed a Gaussian alternation with different peaks, depending on the disease condition. Previously published data have indicated the same order of magnitude for the elastic moduli of cells through nanoindentation.[14,31] The K-means clustering centers showed 400, 1000, 1300, and 3700 Pa for cellular parts of serous, endometriosis, mucinous, and mature tumors, respectively, with the highest relative frequency in the cellular histogram parts (Figure 4A–D). The cellular part in serous cystadenoma was highly soft, with the average of 400 Pa, which was more than two and three folds softer than endometriosis and mucinous cystadenoma, respectively. The average elastic moduli of cellular parts were 1000 Pa for endometriosis and 1300 Pa for mucinous one; however, the cells in mature teratoma showed by far higher elasticity, with the average of 3700 Pa. An ANOVA statistical measurement indicated that the difference between cellular profiles in quantified diseases was statistically significant ($P<0.05$), with the exception of difference between endometriosis and mucinous tumors (Figure 5A).

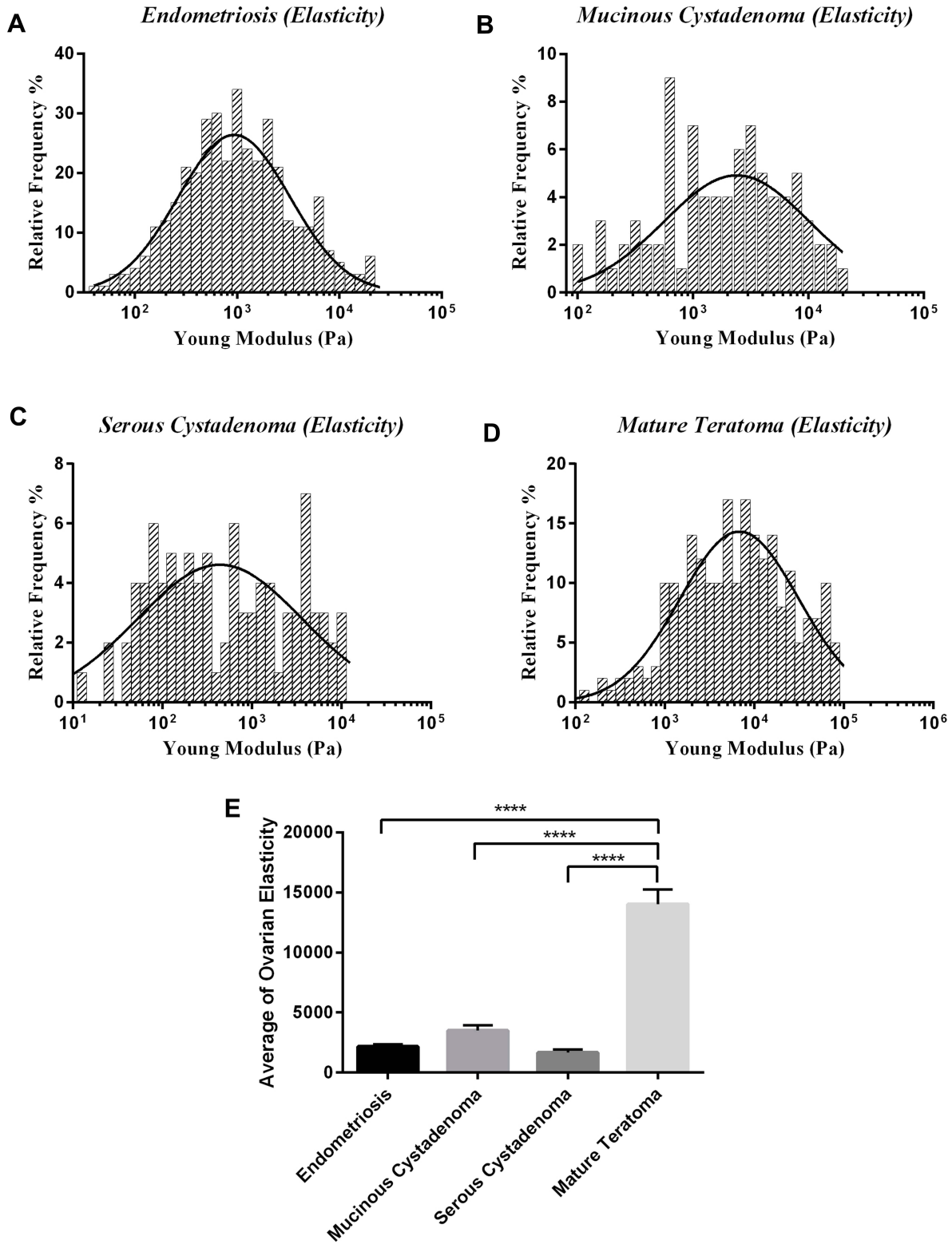

Figure 2 Represents Young's modulus histogram of tissues of different ovarian diseases in logarithmic scale with a Gaussian distribution plot fitted on histograms. (**A**) Endometriosis, (**B**) mucinous cystadenoma, (**C**) serous cystadenoma, (**D**) mature teratoma, and (**E**) the average elastic moduli of ovarian tissues with four diseases. Measurements were carried out by atomic force microscopy in force spectroscopy mode at room temperature under physiological conditions. The significant differences in parameters of test groups were reported with the * sign (****p<0.0001).

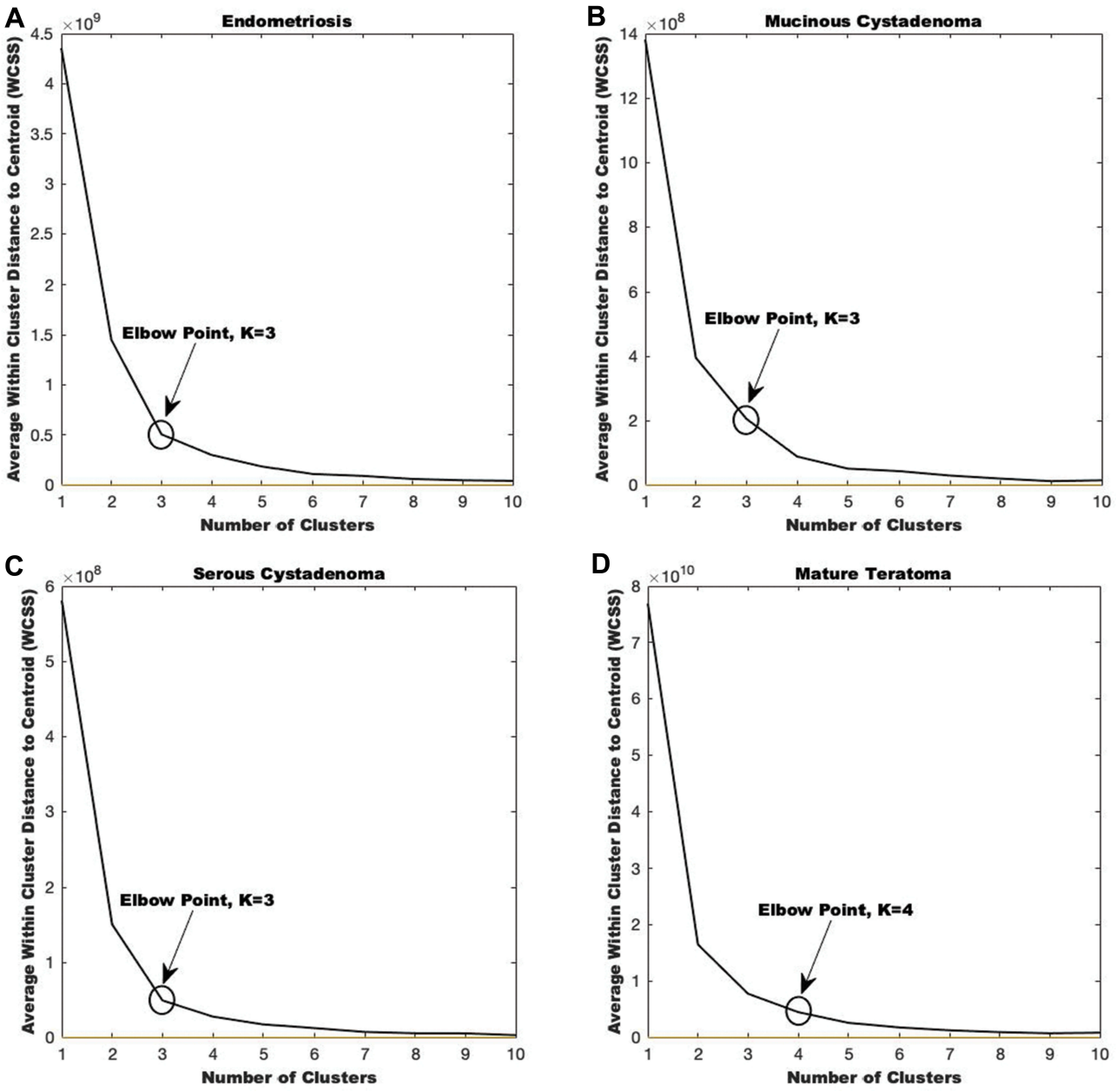

Figure 3 Obtaining number of clusters by elbow methods. Figure represents average within the cluster distance of elasticity profiles of indented tissues four ovarian diseases versus the clustering number. (**A**) Elbow method for endometriosis. (**B**) Elbow method for mucinous cystadenoma. (**C**) Elbow method for serous cystadenoma. (**D**) Elbow method for mature teratoma. Results were further verified by silhouette method.

The data of elastic moduli were sorted in different partitions of cellular, soft ECM, rigid ECM, and highly rigid ECM. The extracellular matrix in mature teratoma is by far stiffer than other disorders, with elastic moduli of 17 kPa for the soft ECM components and 40 kPa and 66 kPa for rigid and highly rigid ones. Unlike the mature teratoma tissue, the average value for the softest quantified tissue, serous cystadenoma, is roughly 4 kPa for the soft ECM and 10 kPa for the rigid ECM components. For endometriosis and mucinous ovarian samples, the elastic modulus of ECM soft regions was approximately 6 kPa for both tissues. Endometriosis showed the second highest rigid ECM (ECMr) with the elastic modulus value of 18 kPa (Figure 5B and C). With combining the data of all ECM types (non-cellular parts), the average value for elastic moduli was measured 31 kPa, 8 kPa, 8 kPa, and 5 kPa for mature teratoma, endometriosis, mucinous, and serous ovarian tissues, respectively, with the significant differences between mature teratoma and other quantified diseases ($P<0.05$) (Figure 5D). Generally, there were unnoticeable differences in elastic moduli of both

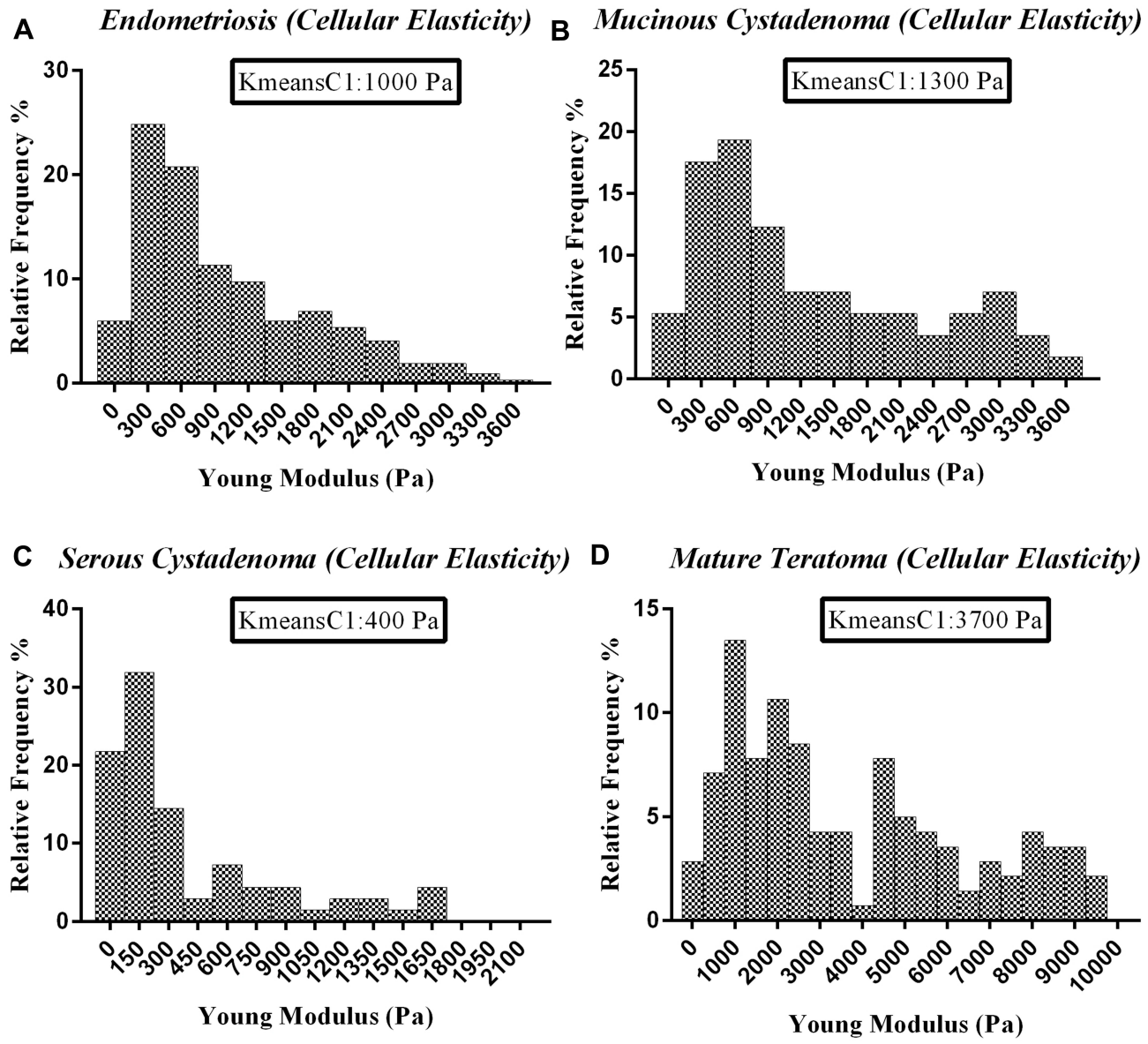

Figure 4 Represents the cellular elasticity profiles of ovarian tissues of four different diseases measured by atomic force microscopy. (**A**) Endometriosis, (**B**) mucinous cystadenoma, (**C**) serous cystadenoma, (**D**) mature teratoma. K-means clustering was applied to categorize elasticity data. K-means clustering center 1 (kmeanC1) represents the clustering center of cellular region which significantly depends on the disease condition.

cellular and ECM components, when endometriosis tissues with mucinous tumors were compared (P>0.05), while samples of two other diseases showed significant alternations in both parts (Figure 5A–D).

The histological images of sections of ovarian samples with four diseases are shown in Figures 6 and 7 All samples show a diverse range of objects specially among the non-cellular parts. This might be the cause for categorizing elastic moduli of ECM in two or three separate categories. The cellular parts include different cells such as epithelial cells and fibroblasts. The non-cellular parts include both fibrous (mostly collagenous) and non-fibrous zones, in which the latter includes a wide range of tissues such as endometrial and sebaceous glands, adipose tissue, vessel walls, mucinous layer, and keratin layer depending on the disease. Such variety of objects define a wide range of elastic moduli, with higher moduli than that of cell body, yet lower than that of fibrous ECM. Hence, the non-cellular part represents at least two distinct ranges of elastic moduli, most likely due to fibrous and non-fibrous structures.

Discussion

Cells set the function of tissues through multiple behaviors such as migration, proliferation, synthesis, and regulation

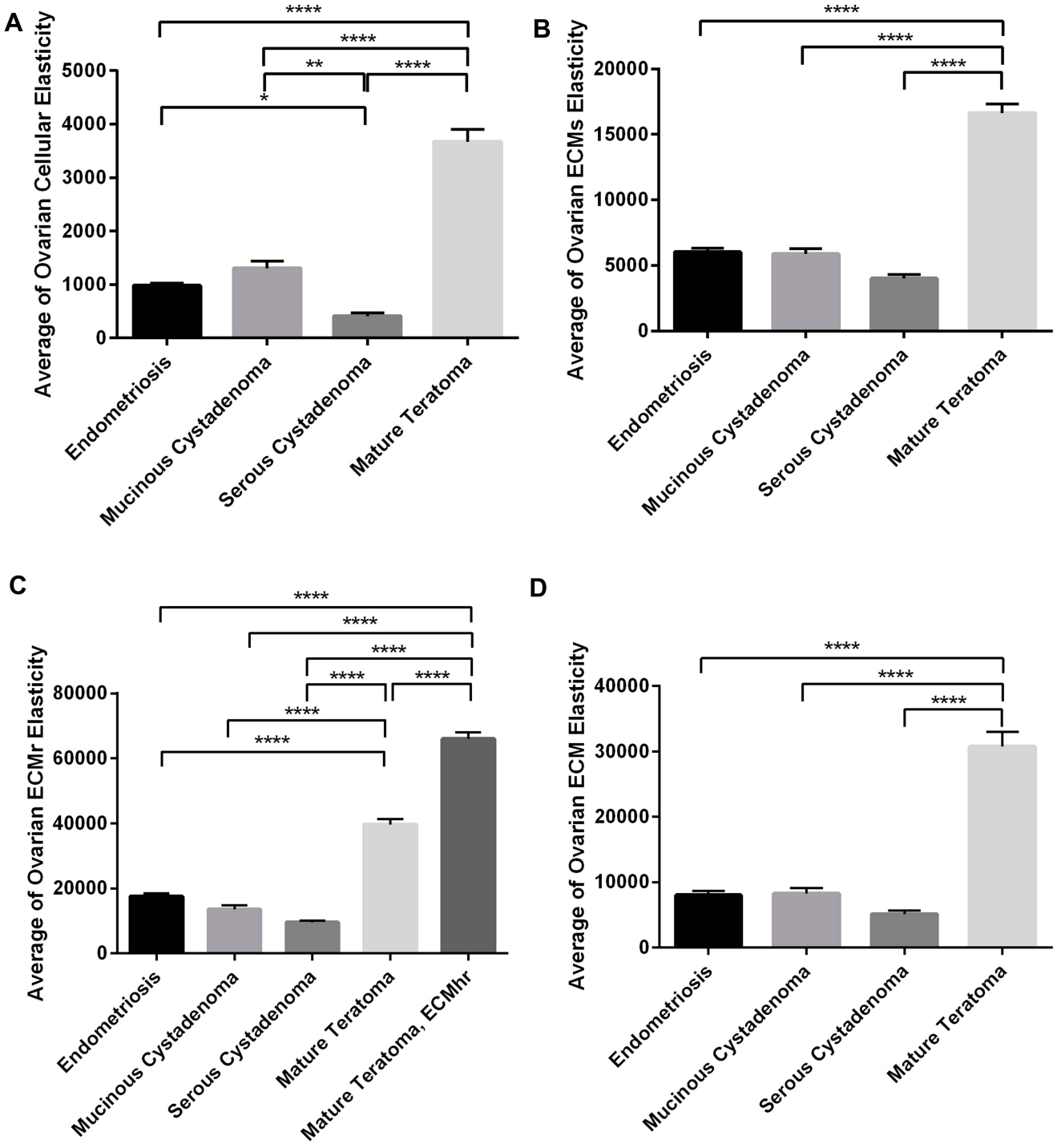

Figure 5 Represents the average elastic moduli of cellular and ECM parts of quantified diseases. (**A**) Cellular and (**B–D**) extracellular matrix portions. Bonferroni's multiple comparison test was performed to compare data statistically. The significant differences in parameters of test groups were reported with the *sign (*p<0.05, **p<0.01, and ****p<0.0001).

of ECM by which the dynamic state of homeostasis is met. Mutually, chemical and physical environmental stimuli influence cells through ECM and further regulate cell behaviors. The interactive process of cell-ECM signaling defines and guides biological processes in tissue level such as morphogenesis, tissue remodeling, healing, and disease development. During initiation and progression of diseases, the properties of both cell and ECM including their physical properties change. Alterations in mechanical properties of both cell bodies and ECM are due to altered

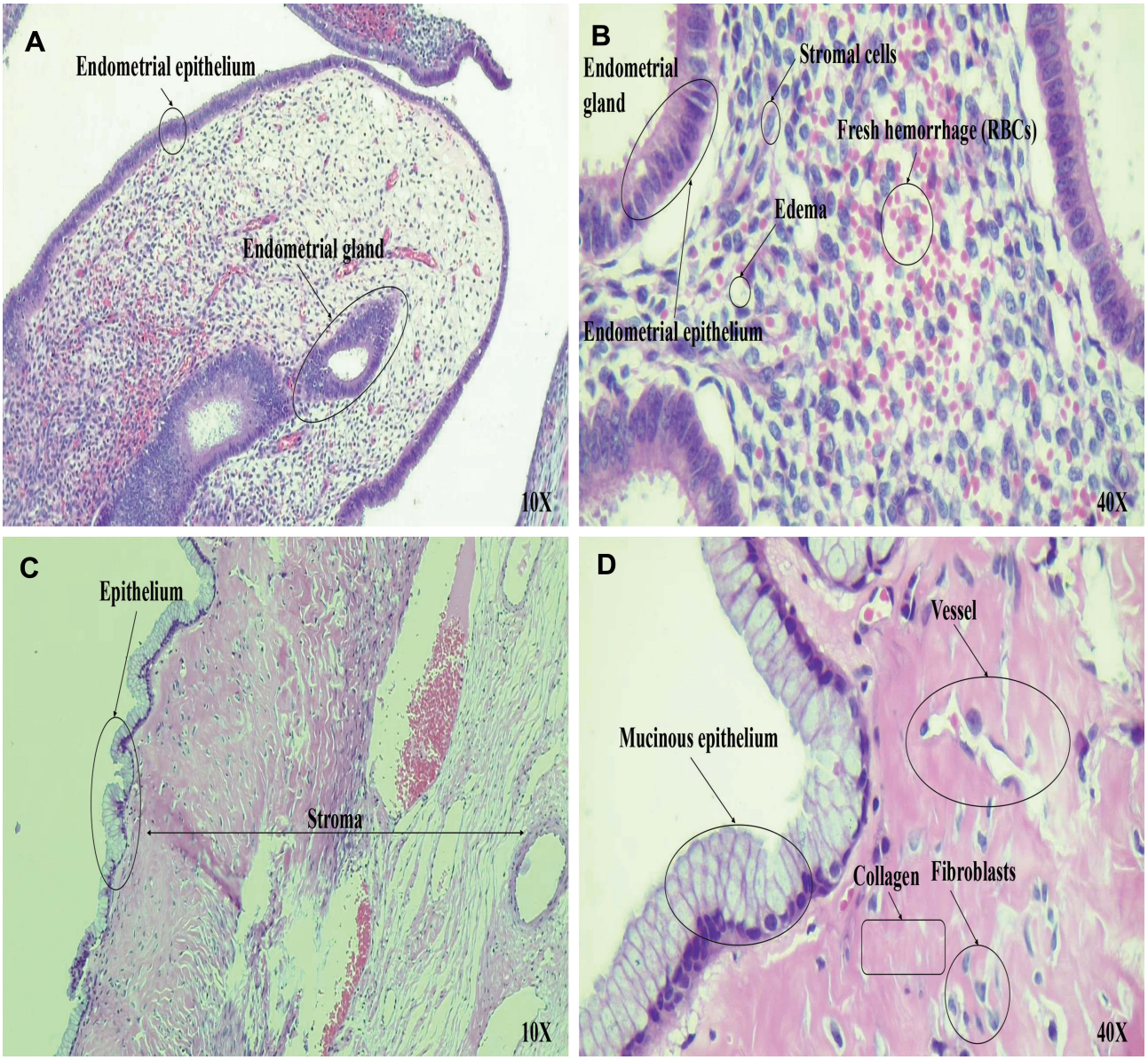

Figure 6 Histopathological examination of ovarian tissues. (**A** and **B**) Microscopic examination of hematoxylin and eosin (H&E) stained sections demonstrate endometriosis. (**A**) Microscopic low power examination (10×) reveals ovarian cyst lined by endometrial glands and decasualized stroma is evident. Hemosiderin laden macrophages and features of old hemorrhage are also seen. (**B**) High-power examination (40×) of the stromal cells shows abundant eosinophilic cytoplasm, distinct cell membrane, and round uniform nuclei consistent with progesterone hormonal effect on the underlying endometriosis. (**C** and **D**) Microscopic examination of hematoxylin and eosin (H&E) stained sections demonstrate mucinous cystadenoma. (**C**) Microscopic low power examination (10×) shows ovarian tissue with cystic structure, fibrotic stroma and (**D**) microscopic high-power examination (40×) shows a flat mucinous epithelial lining, without significant atypia compatible with mucinous cystadenoma.

structural arrangement and/or content of fibrous components which remodel cell cytoskeleton and ECM synthesis and degradation. The extent of such alterations is such that, these changes have been proposed as biomarkers of diseases, most notably in cancer.[63] It has been well established that cancer cells are softer than normal cells while the ECM of cancerous tissues is stiffer, and these alterations are intensified by increased invasion.[2,64] Cancerous cells are highly deformable, especially during invasion, to penetrate tissue matrix and migrate to implement intravasation and extravasation by which they pass through endothelial junctions of vessel walls and reach the bloodstream and with the same pattern penetrate to a new tissue and metastasize.[65] Cancer cells also affect ECM to facilitate their migration by degradation through secretion of abnormal MMPs and synthesis and rearrangement of a new fibrous structure.[66] It seems that during initiation and progress of many pathological conditions, cellular and non-cellular parts of diseased tissues undergo remodeling which causes altered mechanical properties for

new biological conditions.[67] Here, we examined the differences among cellular and non-cellular parts of ovarian-related tumorigenic and non-tumorigenic diseases and found significant differences among elastic moduli of those parts.

Tissues related to four non-malignant ovarian diseases, mucinous cystadenoma, serous cystadenoma, and mature teratoma, as tumorous diseases, and endometriosis, as the non-tumorous disease, had different mechanical properties both in terms of cellular and non-cellular elastic moduli depending on the disease condition. On average, samples of mature teratoma showed the stiffest microenvironment and were approximately six times stiffer than samples of serous cystadenoma (the softest) in ECM region and nearly nine folds stiffer in cellular region (Figure 5A and D). Such quantities show the wide extent of variation in mechanical properties of biological tissues in different disease conditions, as cells comply to the pathological state by remodeling their behavior which affects their structures, most likely through their cytoskeleton, as well as ECM rearrangement.[68]

It has been shown that some benign ovarian tumors of mucinous or serous origins can potentially be transformed to malignant state.[69,70] A majority of low-grade invasive serous ovarian carcinomas coexist with ovarian tumors of micropapillary and typical types, which in turn usually coexist with serous borderline tumors.[71,72] The overexpression and mutation of p53 marker, which is highly related to the carcinomas, were also detected in ovarian benign tumors.[73,74] Furthermore, it has been suggested that the risk of several types of ovarian cancer increases among women with endometriosis.[75] Moreover, although mature cystic teratoma hardly undergoes malignant transformation, the possibility of such incidence increases with age.[76–78] Overall, the close relations between ovarian benign lesions and carcinoma incidences highlight the importance of study of benign lesion microenvironment. Our results indicated that different ovarian benign lesions have undergone significant alterations according to their pathological states, with highest variations in their ECM elasticity most probably due to cell remodeling which affects ECM synthesis and regulation. Cells of these tissues also showed different elastic properties. The high heterogeneity among cell and ECM parts of samples with different disease states indicates the high impact of pathological conditions of microenvironment on tissue mechanical properties which can assist in the understanding of development of these conditions. It might seem at first that softer benign cells produce softer ECMs; however, there is no biological evidence for this. During cancer onset and development, cancer cells undergo softening with invasion degree, while ECM becomes stiffer.[65] Here, although for samples with mature teratoma both cellular and non-cellular zones are significantly stiffer than those of other samples, there is no such trend when samples of other three benign conditions are compared. In other words, the trend of stiffening of cellular parts does not match the trends among ECMr and ECMs regions of samples of endometriosis, mucinous cystadenoma, and serous cystadenoma, and their properties depend on disease conditions. Each pathological state indicates a specific structural property of cells and ECM parts to meet the requirements of that disease. Hence, since ECM changes are due to cell behaviors, there is a correlation between cellular and ECM microenvironment elasticity; however, such correlation varies among different diseases and possibly among different stages of the disease. The cystic environments of the mucinous and serous are different which may affect both cellular and ECM microenvironments. The cyst of serous contains watery fluid or occasionally thin mucinous fluid compared to that of mucinous cystadenoma which is filled with thick mucoid material.[79] In this regard, the physiological conditions of serous cyst, having unilocular lesions and homogenous microenvironment with a thin regular wall may influence alternation of elasticity histograms, leading to decreasing ranges of both cellular and ECM elasticity variations. However, mucinous cysts are multilocular cystic structures, with cytoplasm containing abundant mucin materials and fibro collagenous stroma with variable cellularity. These futures lead to having both stiffer cells and ECM in mucinous tumors compared to the serous one (Figure 5A–D).[80,81]

Our results indicated a wide range of elastic moduli among samples of ovarian tissues shown in the elasticity histograms (Figure 2A–D). Such range of data defined elastic properties of both cellular and non-cellular regions. Since non-cellular regions are stiffer in nature than the cellular parts, we intended to divide data into categories to distinguish between cellular and non-cellular parts. This allows to obtain average values of elastic moduli of different regions and compare those among samples of several diseases. AFM technique is able to probe very locally; however, the histological evaluation is not feasible during indentation such that there is no sufficient resolution to distinguish between the individual tissue components.[65,82] Hence, we used clustering algorithms that "naturally" categorize data into a suitable number of categories with

the highest similarity among data of each group and the least similarity between groups without subjective intervention. The coordination of measurements during AFM for elasticity quantification was also used to investigate the nature of probed local tissue by H&E staining of examined sections (Figures 6 and 7). Previously we used Fuzzy C-means method to distinguish between elastic moduli of cellular and non-cellular zones among samples of normal and cancerous breast tissues and found that the cellular parts of cancerous tissues were significantly softer than those of healthy tissues.[4] We distinguished three categories to cluster data of breast tissues. We named them as cellular region, intermediate region containing less dense ECM fibers together with ducts and lumens, and fibrous ECM region. In this study, we used two methods of K-means and fuzzy C-means in parallel with similar results in indentation data clustering, demonstrating the high similarity of these two clustering methods in our study. Similarly, here we distinguished three regions among samples of three diseases and named them as cellular part, ECM soft region (ECMs), and ECM rigid one (ECMr). For the tumorous mature teratoma samples, the non-cellular part was categorized with one more region of extra stiff fibrous zone. Similar to our previous work, variations among less fibrous part of ECM were lower compared to the denser and more fibrous parts (Figure 5B and C). When the non-cellular parts among study groups were averaged (Figure 5D), data revealed that on average, the non-cellular parts of samples of different diseases were 7 to 10 times stiffer than the cellular part (Figure 5A and D).

Teratomas may include not only the rudiments of a variety of tissues but also organs and groups of organs. In mature teratomas, derivatives of germ layers can differentiate up to very impressive and even artistic levels described as "fetus in the fetu", and mitotic activity in them is either absent or only slightly expressed.[76] The most common ectodermal components in them include the skin epidermis, pilosebaceous structures, sweat glands, teeth, and neurological tissues. Mesoderm is most commonly represented by cartilage, bone, fat, and muscle (smooth and striated) tissue, and endoderm is represented by cysts lined with respiratory and intestinal epithelium, and sometimes parts of the pancreas and liver.[83] In this trend, differentiation to different organs is the dominant feature of these tumors.[79,84] Interestingly, it has been shown that the wide range of elasticity in these tissues can serve as a mechanical stimulation to induce differentiation potential in cells to the different target cells depending highly on the mechanical microenvironment.[25,85,86] Our results also confirm this trend, as the range of elasticity histogram in mature teratoma samples was almost four times higher than those of other diseases and showed a marked mechanical heterogeneity through the tissue sections, in such that we defined three ECM related zones of different elastic moduli with natural clustering of data (Figure 3). Such broad range was also observed in cellular region among three pathological states, which is a confirmation in existence of different types of cells related to the disease condition (Figure 4A–D).

Endometriosis is considered as a non-tumorous ovarian disorder and we studied samples of these tissues to compare with other ovarian tumor-based diseases. Similar to tumorous ovarian tissues, these samples also showed variations in mechanical properties among cellular and ECM portions and showed different mechanical properties from tumorous ovarian tissues, particularly, their cells were significantly stiffer than serous cystadenoma cells and softer than mature teratoma cells. Both serous cystadenoma and mature teratoma have markedly higher cancer incidences than mucinous cystadenoma. Almost 90% of ovarian cancers involve epithelial cells, among which serous carcinoma cases are the most abundant with 52% of cases and mucinous carcinoma the least common with only 6% of cases.[87] The very soft nature of serous carcinoma cells might contribute to a majority of cancer-related events in ovarian tissue and can be considered for therapeutic actions.[88–90] The highly deformable cells can swiftly migrate through ECM, pass endothelial junctions, endure shearing forces of the blood flow, and settle in a new tissue. Accordingly, results indicated that serous carcinoma cells, with higher likelihood of becoming malignant, are significantly softer than cells of all other three ovarian diseases ($P<0.05$) (Figure 5A). The histological images of diseased tissues show a considerable level of fibroblasts which are also another source of cells in tissues that contribute to the elasticity of cellular part of samples. Interestingly, cancer onset and progress is accompanied by the cross-talks between cancerous epithelial cells and cancer-associated fibroblasts (CAFs) which facilitate the process of detachment from tumor, ECM degradation, and further synthesis and migration.[91]

It seems that among samples of ovarian tissues with four diseases, the fibrous parts of the ECM represent the higher range of elasticity (represented by ECMr in Figure 5C), while the non-fibrous parts characterize the softer elasticity

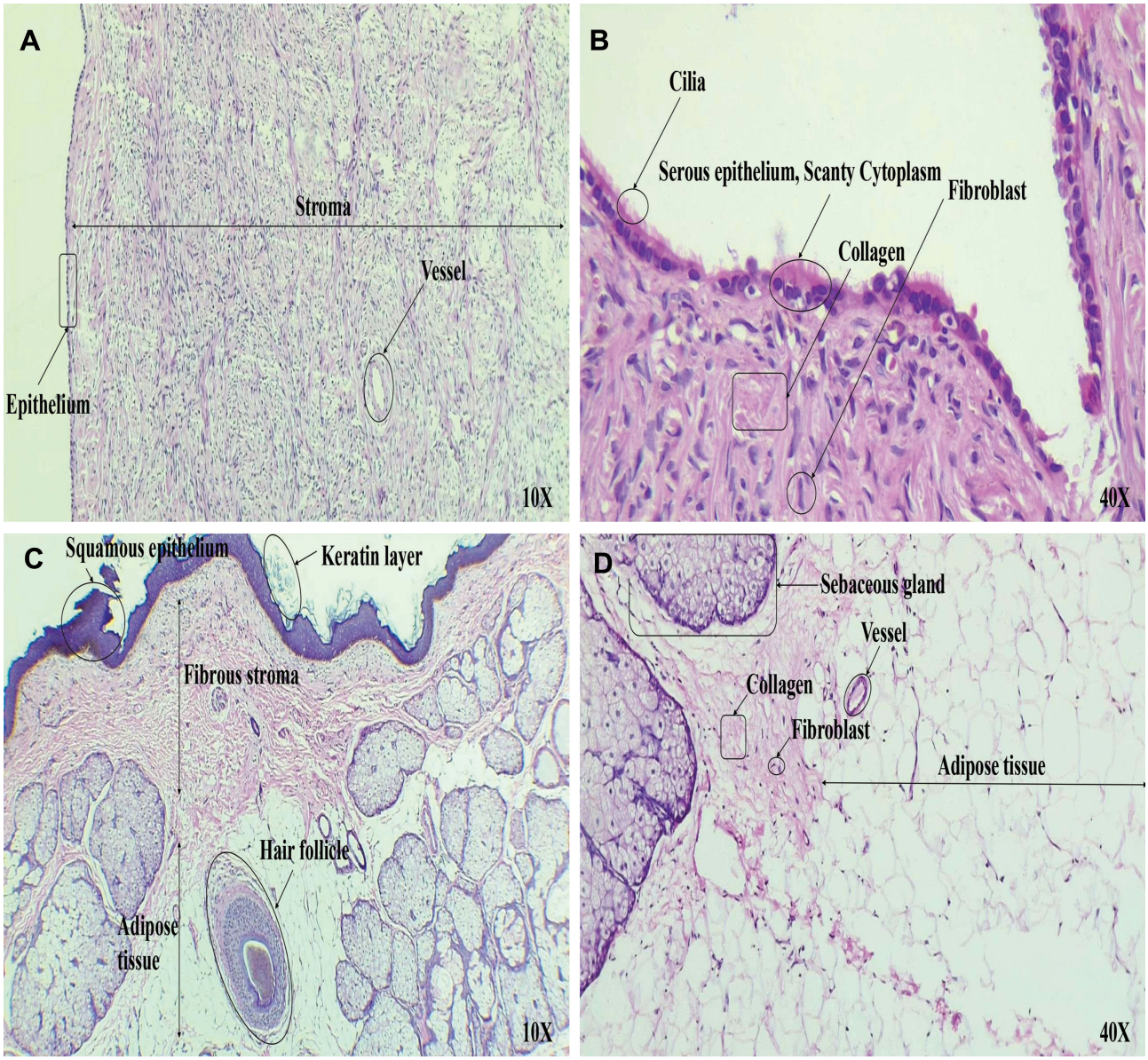

Figure 7 Histopathological examination of ovarian tissues. (**A** and **B**) Microscopic examination of hematoxylin and eosin (H&E) stained sections demonstrate serous cystadenoma. (**A**) Microscopic low power examination (10×) shows ovarian tissue with fibrotic stroma and multiple cystic structures. (**B**) Microscopic high-power examination (40×) depicts that the tissue sections were lined with flat or cuboidal ciliated epithelial cells without significant atypia compatible with serous cystadenoma. (**C** and **D**) Microscopic examination of hematoxylin and eosin (H&E) stained sections demonstrate mature teratoma. (**C**) Microscopic low power examination (10×) reveals ovarian cyst with keratinizing squamous epithelial lining, normal skin appendices, and hair follicle consistent with mature teratoma. (**D**) High-power examination (40×) reveals a mature adipose tissue (at the bottom) and sebaceous gland (left of the figure) are seen.

range (described by ECMs in Figure 5B). Samples of mature teratoma possess dense collagenous fibrous locations which are most likely related to the stiffest ECM part of samples (represented by ECMhr). While the non-fibrous part contains a variety of tissues among all samples of different diseases, the highly diverse range of objects in the samples of mature teratoma includes even more objects such as adipose tissue, sebaceous gland, hair follicle, keratin layer, vessel wall, fibrous stroma, and dense collagen fibers. This necessitates a higher number of categories of ECM elastic modulus compared to tissues of other three diseases. Hence, using a clustering algorithm, while ECM of other ovarian diseases was naturally categorized by two groups, the ECM of mature teratoma was characterized by three categories with distinct elastic moduli.

In conclusion, tissues which undergo pathological conditions experience variation of mechanical properties among cellular and non-cellular parts. For the ovarian tissue, samples of three tumor-based diseases and one non-tumorous disease revealed marked variations

among all cellular and non-cellular parts including less dense and highly dense ECM portions. It was shown that different diseases have direct effects on changing cellular microenvironment and even on the cell mechanical properties, enhancing the symptoms. Furthermore, these results also represented the ability of AFM to reveal alterations in the tissue structural properties in pathological conditions. Aside from clustering algorithms to categorize tissue content, there are other AFM-based techniques for surveying tissues to distinguish structure and morphology of the indented location that might assist in the study of diseased tissues in future studies, such as force volume imaging which simultaneously provides both morphology and elasticity data.[92] Such approach is rather time-consuming and might result in sample degradation in some cases. Furthermore, it is possible to combine both force spectroscopy and contact modes to probe the 3D morphology of indented material.[11] This technique also is limited in application, since the contact mode requires separate set up with a soft probe that results in rescanning the samples. Another approach which has been used is conjugating the probe tip with specific biomarkers, for molecular recognition approach. Due to high diversity of tissue structure, this application might require different biomarkers including conjugated proteins to probe all cellular and non-cellular content. The possibility of recruiting these techniques after overcoming limitations remains an interesting field of future studies. Our results may be assistive in the study of physical microenvironment of cells during onset and progress of diseases and their correlation with biological events, of particular interest in cancer. Such variations may be quantified as biomarkers in disease initiation and progression and be used in diagnostic tools and treatment strategies.

Disclosure

The authors report no conflicts of interest in this work.

References

1. Kai F, Laklai H, Weaver VM. Force matters: biomechanical regulation of cell invasion and migration in disease. *Trends Cell Biol*. 2016;26(7):486–497. doi:10.1016/j.tcb.2016.03.007
2. Alibert C, Goud B, Manneville JB. Are cancer cells really softer than normal cells? *Biol Cell*. 2017;109(5):167–189. doi:10.1111/boc.201600078
3. Kraning-Rush CM, Califano JP, Reinhart-King CA. et al. Cellular traction stresses increase with increasing metastatic potential. *PLoS One*. 2012;7(2):e32572. doi:10.1371/journal.pone.0032572
4. Ansardamavandi A, Tafazzoli-Shadpour M, Omidvar R, Jahanzad I. Quantification of effects of cancer on elastic properties of breast tissue by atomic force microscopy. *J Mech Behav Biomed Mater*. 2016;60:234–242. doi:10.1016/j.jmbbm.2015.12.028
5. Cross SE, Jin Y-S, Rao J, Gimzewski JK. Nanomechanical analysis of cells from cancer patients. *Nat Nanotechnol*. 2007;2(12):780. doi:10.1038/nnano.2007.388
6. Lekka M. Discrimination between normal and cancerous cells using AFM. *Bionanoscience*. 2016;6(1):65–80. doi:10.1007/s12668-016-0191-3
7. Hayashi K, Iwata M. Stiffness of cancer cells measured with an AFM indentation method. *J Mech Behav Biomed Mater*. 2015;49:105–111. doi:10.1016/j.jmbbm.2015.04.030
8. Pu H, Liu N, Yu J, et al. Micropipette aspiration of single cells for both mechanical and electrical characterization. *IEEE Trans Biomed Eng*. 2019;66(11):3185–3191. doi:10.1109/TBME.2019.2901763
9. Last JA, Russell P, Nealey PF, Murphy CJ. The applications of atomic force microscopy to vision science. *Invest Ophthalmol Vis Sci*. 2010;51(12):6083–6094. doi:10.1167/iovs.10-5470
10. Lin C, Liu Y, Xie X. GO/PVA nanocomposites with significantly enhanced mechanical properties through metal ion coordination. *Chin Chem Lett*. 2019;30(5):1100–1104. doi:10.1016/j.cclet.2018.11.027
11. Li H, Xie X-M. Polyolefin-functionalized graphene oxide and its GO/HDPE nanocomposite with excellent mechanical properties. *Chin Chem Lett*. 2018;29(1):161–165. doi:10.1016/j.cclet.2017.06.001
12. Kumar S, Weaver VM. Mechanics, malignancy, and metastasis: the force journey of a tumor cell. *Cancer Metastasis Rev*. 2009;28(1–2):113–127. doi:10.1007/s10555-008-9173-4
13. Plodinec M, Loparic M, Monnier CA, et al. The nanomechanical signature of breast cancer. *Nat Nanotechnol*. 2012;7(11):757. doi:10.1038/nnano.2012.167
14. Lekka M, Gil D, Pogoda K, et al. Cancer cell detection in tissue sections using AFM. *Arch Biochem Biophys*. 2012;518(2):151–156. doi:10.1016/j.abb.2011.12.013
15. Lin -H-H, Lin H-K, Lin I-H, et al. Mechanical phenotype of cancer cells: cell softening and loss of stiffness sensing. *Oncotarget*. 2015;6(25):20946. doi:10.18632/oncotarget.4173
16. Torre LA, Trabert B, DeSantis CE, et al. Ovarian cancer statistics, 2018. *CA Cancer J Clin*. 2018;68(4):284–296. doi:10.3322/caac.21456
17. Canato M, Dal Maschio M, Sbrana F, et al. Mechanical and electrophysiological properties of the sarcolemma of muscle fibers in two murine models of muscle dystrophy: col6a1−/− and mdx. *Biomed Res Int*. 2010;2010.
18. Janmey PA, Miller RT. Mechanisms of mechanical signaling in development and disease. *J Cell Sci*. 2011;124(1):9–18. doi:10.1242/jcs.071001
19. Assoian RK, Klein EA. Growth control by intracellular tension and extracellular stiffness. *Trends Cell Biol*. 2008;18(7):347–352. doi:10.1016/j.tcb.2008.05.002
20. Fattovich G, Stroffolini T, Zagni I, Donato F. Hepatocellular carcinoma in cirrhosis: incidence and risk factors. *Gastroenterology*. 2004;127(5):S35–S50. doi:10.1053/j.gastro.2004.09.014
21. Wood CD, Vijayvergia M, Miller FH, et al. Multi-modal magnetic resonance elastography for noninvasive assessment of ovarian tissue rigidity in vivo. *Acta Biomater*. 2015;13:295–300. doi:10.1016/j.actbio.2014.11.022
22. Burleson KM, Casey RC, Skubitz KM, Pambuccian SE, Jr TR O, Skubitz AP. Ovarian carcinoma ascites spheroids adhere to extracellular matrix components and mesothelial cell monolayers. *Gynecol Oncol*. 2004;93(1):170–181. doi:10.1016/j.ygyno.2003.12.034
23. Zhang Y, He Y, Bharadwaj S, et al. Tissue-specific extracellular matrix coatings for the promotion of cell proliferation and maintenance of cell phenotype. *Biomaterials*. 2009;30(23–24):4021–4028. doi:10.1016/j.biomaterials.2009.04.005
24. Justin RT, Engler AJ. Stiffness gradients mimicking in vivo tissue variation regulate mesenchymal stem cell fate. *PLoS One*. 2011;6(1):e15978. doi:10.1371/journal.pone.0015978

25. Watt FM, Huck WT. Role of the extracellular matrix in regulating stem cell fate. *Nat Rev Mol Cell Biol*. 2013;14(8):467. doi:10.1038/nrm3620
26. Zemła J, Stachura T, Gross-Sondej I, et al. AFM-based nanomechanical characterization of bronchoscopic samples in asthma patients. *J Mol Recognit*. 2018;31(12):e2752. doi:10.1002/jmr.2752
27. Suki B, Bates JH. Extracellular matrix mechanics in lung parenchymal diseases. *Respir Physiol Neurobiol*. 2008;163(1–3):33–43. doi:10.1016/j.resp.2008.03.015
28. Moon HJ, Sung JM, Kim E-K, Yoon JH, Youk JH, Kwak JY. Diagnostic performance of gray-scale US and elastography in solid thyroid nodules. *Radiology*. 2012;262(3):1002–1013. doi:10.1148/radiol.11110839
29. Rago T, Vitti P. Role of thyroid ultrasound in the diagnostic evaluation of thyroid nodules. *Best Pract Res Clin Endocrinol Metab*. 2008;22(6):913–928. doi:10.1016/j.beem.2008.09.016
30. Rebelo LM, de Sousa JS, Mendes Filho J, Radmacher M. Comparison of the viscoelastic properties of cells from different kidney cancer phenotypes measured with atomic force microscopy. *Nanotechnology*. 2013;24(5):055102. doi:10.1088/0957-4484/24/5/055102
31. Lekka M, Pogoda K, Gostek J, et al. Cancer cell recognition–mechanical phenotype. *Micron*. 2012;43(12):1259–1266. doi:10.1016/j.micron.2012.01.019
32. Herek D, Karabulut A, Agladioglu K. Usefulness of transabdominal real-time sonoelastography in the evaluation of ovarian lesions: preliminary results. *Br J Radiol*. 2016;89(1065):20160173. doi:10.1259/bjr.20160173
33. Prat J, Cao D, Carinelli S, Nogales F, Vang R, Zaloudek C. Who Classification of Tumours of Female Reproductive Organs. *Lyon*:2014.
34. Stany MP, Hamilton CA. Benign disorders of the ovary. *Obstet Gynecol Clin North Am*. 2008;35(2):271–284. doi:10.1016/j.ogc.2008.03.004
35. Sofoudis C, Vassiliadou D, Georgoulias G, Papamargaritis E, Gerolymatos A. Mixed Benign Ovarian Neoplasms: a Report of Five Cases. *Mixed Benign Ovarian Neoplasms*. 2018;1:1–7.
36. Hollis RL, Gourley C, L Hollis R, Gourley C. Genetic and molecular changes in ovarian cancer. *Cancer Biol Med*. 2016;13(2):236. doi:10.20892/j.issn.2095-3941.2016.0024
37. Matulonis UA, Sood AK, Fallowfield L, Howitt BE, Sehouli J, Karlan BY. Ovarian cancer. *Nat Rev Dis Primers*. 2016;2(1):16061. doi:10.1038/nrdp.2016.61
38. Harrison M, Jameson C, Gore M. Mucinous ovarian cancer. *Int J Gynecological Cancer*. 2008;18(2):209–214.
39. Brown J, Frumovitz M. Mucinous tumors of the ovary: current thoughts on diagnosis and management. *Curr Oncol Rep*. 2014;16(6):389. doi:10.1007/s11912-014-0389-x
40. Peterson WF, Prevost EC, Edmunds FT, Hundley JM, Morris FK. Benign cystic teratomas of the ovary: a clinico-statistical study of 1007 cases with a review of the literature. *Am J Obstet Gynecol*. 1955;70(2):368–382. doi:10.1016/S0002-9378(16)37681-5
41. Roth LM, Talerman A. Recent advances in the pathology and classification of ovarian germ cell tumors. *Int j Gynecological Pathol*. 2006;25(4):305–320. doi:10.1097/01.pgp.0000225844.59621.9d
42. Kobayashi H, Sugimoto H, Onishi S, Nakano K. Novel biomarker candidates for the diagnosis of ovarian clear cell carcinoma. *Oncol Lett*. 2015;10(2):612–618. doi:10.3892/ol.2015.3367
43. Barrett CL, DeBoever C, Jepsen K, Saenz CC, Carson DA, Frazer KA. Systematic transcriptome analysis reveals tumor-specific isoforms for ovarian cancer diagnosis and therapy. *Proc National Acad Sci*. 2015;112(23):E3050–E3057. (). doi:10.1073/pnas.1508057112
44. Bhadriraju K, Hansen LK. Extracellular matrix-and cytoskeleton-dependent changes in cell shape and stiffness. *Exp Cell Res*. 2002;278(1):92–100. doi:10.1006/excr.2002.5557
45. Howard D. *The Role of the Cytoskeleton in Alzheimer's Disease: A Drosophila Perspective*. United Kingdom: The University of Manchester; 2016.
46. Williams JR. The Declaration of Helsinki and public health. *Bull World Health Organ*. 2008;86(8):650–652. doi:10.2471/BLT.08.050955
47. Engler AJ, Griffin MA, Sen S, Bönnemann CG, Sweeney HL, Discher DE. Myotubes differentiate optimally on substrates with tissue-like stiffness: pathological implications for soft or stiff microenvironments. *J Cell Biol*. 2004;166(6):877–887. doi:10.1083/jcb.200405004
48. Puttini S, Lekka M, Dorchies OM, et al. Gene-mediated restoration of normal myofiber elasticity in dystrophic muscles. *Mol Ther*. 2009;17(1):19–25. doi:10.1038/mt.2008.239
49. Levy R, Maaloum M. Measuring the spring constant of atomic force microscope cantilevers: thermal fluctuations and other methods. *Nanotechnology*. 2001;13(1):33. doi:10.1088/0957-4484/13/1/307
50. Wu P-H, Aroush DR-B, Asnacios A, et al. A comparison of methods to assess cell mechanical properties. *Nat Methods*. 2018;15(7):491–498. doi:10.1038/s41592-018-0015-1
51. Ding Y, Wang J, Xu G-K, Wang G-F. Are elastic moduli of biological cells depth dependent or not? Another explanation using a contact mechanics model with surface tension. *Soft Matter*. 2018;14(36):7534–7541. doi:10.1039/C8SM01216D
52. Faria EC, Ma N, Gazi E, et al. Measurement of elastic properties of prostate cancer cells using AFM. *Analyst*. 2008;133(11):1498–1500. doi:10.1039/b803355b
53. Li M, Liu L, Xi N, Wang Y. Research progress in quantifying the mechanical properties of single living cells using atomic force microscopy. *Chin Sci Bull*. 2014;59(31):4020–4029. doi:10.1007/s11434-014-0581-2
54. Nikkhah M, Strobl JS, Schmelz EM, Agah M. Evaluation of the influence of growth medium composition on cell elasticity. *J Biomech*. 2011;44(4):762–766. doi:10.1016/j.jbiomech.2010.11.002
55. Ozkan AD, Topal AE, Dana A, Guler MO, Tekinay AB. Atomic force microscopy for the investigation of molecular and cellular behavior. *Micron*. 2016;89:60–76. doi:10.1016/j.micron.2016.07.011
56. Evers FT, Höppner F, Klawonn F, Kruse R, Runkler T. *Fuzzy Cluster Analysis: Methods for Classification, Data Analysis and Image Recognition*. John Wiley & Sons; 1999.
57. Kodinariya TM, Makwana PR. Review on determining number of Cluster in K-Means Clustering. *Int J*. 2013;1(6):90–95.
58. Milligan GW, Cooper MC. An examination of procedures for determining the number of clusters in a data set. *Psychometrika*. 1985;50(2):159–179. doi:10.1007/BF02294245
59. Syakur M, Khotimah B, Rochman E, Satoto B. Integration K-means clustering method and elbow method for identification of the best customer profile cluster. Paper presented at: IOP Conference Series: materials Science and Engineering. 2018.
60. Subbalakshmi C, Krishna GR, Rao SKM, Rao PV. A method to find optimum number of clusters based on fuzzy silhouette on dynamic data set. *Procedia Comput Sci*. 2015;46:346–353. doi:10.1016/j.procs.2015.02.030
61. Fischer AH, Jacobson KA, Rose J, Zeller R. Hematoxylin and eosin staining of tissue and cell sections. *Cold Spring Harb Protoc*. 2008;2008(5):pdb.prot4986. doi:10.1101/pdb.prot4986
62. Feldman AT, Wolfe D. Tissue processing and hematoxylin and eosin staining. In: *Histopathology*. Springer; 2014:31–43.
63. Socovich AM, Naba A The cancer matrisome: from comprehensive characterization to biomarker discovery. Paper presented at: Seminars in cell & developmental biology2019.
64. Wullkopf L, West A-KV, Leijnse N, et al. Cancer cells' ability to mechanically adjust to extracellular matrix stiffness correlates with their invasive potential. *Mol Biol Cell*. 2018;29(20):2378–2385. doi:10.1091/mbc.E18-05-0319
65. Suresh S. Biomechanics and biophysics of cancer cells. *Acta Mater*. 2007;55(12):3989–4014. doi:10.1016/j.actamat.2007.04.022
66. Itoh Y, Nagase H. Matrix metalloproteinases in cancer. *Essays Biochem*. 2002;38:21–36. doi:10.1042/bse0380021

67. Lu P, Takai K, Weaver VM, Werb Z. Extracellular matrix degradation and remodeling in development and disease. *Cold Spring Harb Perspect Biol*. 2011;3(12):a005058. doi:10.1101/cshperspect.a005058
68. Humphrey JD, Dufresne ER, Schwartz MA. Mechanotransduction and extracellular matrix homeostasis. *Nat Rev Mol Cell Biol*. 2014;15(12):802. doi:10.1038/nrm3896
69. Bell DA. Origins and molecular pathology of ovarian cancer. *Mod Pathol*. 2005;18(S2):S19. doi:10.1038/modpathol.3800306
70. Guleria S, Jensen A, Kjær SK. Risk of borderline ovarian tumors among women with benign ovarian tumors: A cohort study. *Gynecol Oncol*. 2018;148(1):86–90. doi:10.1016/j.ygyno.2017.11.024
71. Sehdev AES, Sehdev PS, Kurman RJ. Noninvasive and invasive micropapillary (low-grade) serous carcinoma of the ovary: a clinicopathologic analysis of 135 cases. *Am J Surg Pathol*. 2003;27(6):725–736. doi:10.1097/00000478-200306000-00003
72. Slomovitz BM, Caputo TA, Gretz Iii HF, et al. A comparative analysis of 57 serous borderline tumors with and without a noninvasive micropapillary component. *Am J Surg Pathol*. 2002;26(5):592–600. doi:10.1097/00000478-200205000-00005
73. Kmet LM, Cook LS, Magliocco AM. A review of p53 expression and mutation in human benign, low malignant potential, and invasive epithelial ovarian tumors. *Cancer*. 2003;97(2):389–404. doi:10.1002/cncr.11064
74. Hientz K, Mohr A, Bhakta-Guha D, Efferth T. The role of p53 in cancer drug resistance and targeted chemotherapy. *Oncotarget*. 2017;8(5):8921. doi:10.18632/oncotarget.13475
75. Matalliotakis M, Matalliotaki C, Goulielmos GN, et al. Association between ovarian cancer and advanced endometriosis. *Oncol Lett*. 2018;15(5):7689–7692. doi:10.3892/ol.2018.8287
76. Medeiros F, Strickland KC. *Germ Cell Tumors of the Ovary. In: Diagnostic Gynecologic and Obstetric Pathology (Third Edition)*. Elsevier; 2019:949–1010.
77. GADDUCCI A, PISTOLESI S, ME GUERRIERI, COSIO S, FG CARBONE, AG NACCARATO. Malignant Transformation in Mature Cystic Teratomas of the Ovary: case Reports and Review of the Literature. *Anticancer Res*. 2018;38(6):3669–3675. doi:10.21873/anticanres.12644
78. Gadducci A, Guerrieri ME, Cosio S. Squamous cell carcinoma arising from mature cystic teratoma of the ovary: a challenging question for gynecologic oncologists. *Crit Rev Oncol Hematol*. 2019;133:92–98. doi:10.1016/j.critrevonc.2018.10.005
79. Kumar V, Abbas AK, Aster JC. *Robbins Basic Pathology e-Book*. Elsevier Health Sciences; 2017.
80. Kamel RM. A massive ovarian mucinous cystadenoma: a case report. *Reproduct Biol Endocrinol*. 2010;8(1):24. doi:10.1186/1477-7827-8-24
81. Imaoka I, Wada A, Kaji Y, et al. Developing an MR imaging strategy for diagnosis of ovarian masses. *Radiographics*. 2006;26(5):1431–1448. doi:10.1148/rg.265045206
82. Wong CC-L, Gilkes DM, Zhang H, et al. Hypoxia-inducible factor 1 is a master regulator of breast cancer metastatic niche formation. *Proc National Acad Sci*. 2011;108:201113483.
83. Sorokina I, Borzenkova I, Myroshnychenko M, Pliten O, Omelchenko O, Simachova A. Teratomas: features of the morphological structure and localization. *ProcNational Acad Sci*. 2017;(1):54–57.
84. McCluggage WG. Morphological subtypes of ovarian carcinoma: a review with emphasis on new developments and pathogenesis. *Pathology*. 2011;43(5):420–432. doi:10.1097/PAT.0b013e328348a6e7
85. Discher DE, Janmey.YT, Wang Y. Tissue cells feel and respond to the stiffness of their substrate. *Science*. 2005;310(5751):1139–1143. doi:10.1126/science.1116995
86. Oh SH, An DB, Kim TH, Lee JH. Wide-range stiffness gradient PVA/HA hydrogel to investigate stem cell differentiation behavior. *Acta Biomater*. 2016;35:23–31. doi:10.1016/j.actbio.2016.02.016
87. Torre LA, Trabert B, DeSantis CE, et al. Ovarian cancer statistics, 2018. *CA Cancer J Clin*. 2018;68:284–296.
88. Ansardamavandi A, Tafazzoli-Shadpour M, Shokrgozar MA. Behavioral remodeling of normal and cancerous epithelial cell lines with differing invasion potential induced by substrate elastic modulus. *Cell Adh Migr*. 2018;1–17. doi:10.1080/19336918.2018.1475803
89. Spill F, Reynolds DS, Kamm RD, Zaman MH. Impact of the physical microenvironment on tumor progression and metastasis. *Curr Opin Biotechnol*. 2016;40:41–48. doi:10.1016/j.copbio.2016.02.007
90. Ng MR, Brugge JS. A stiff blow from the stroma: collagen cross-linking drives tumor progression. *Cancer Cell*. 2009;16(6):455–457. doi:10.1016/j.ccr.2009.11.013
91. Mayor R, Etienne-Manneville S. The front and rear of collective cell migration. *Nat Rev Mol Cell Biol*. 2016;17(2):97. doi:10.1038/nrm.2015.14
92. Krieg M, Fläschner G, Alsteens D, et al. Atomic force microscopy-based mechanobiology. *Nat Rev Phys*. 2019;1(1):41–57. doi:10.1038/s42254-018-0001-7